

# 5 *Thermodynamics*

## 5.1 Deviations from Equilibrium

Equilibrium is said to exist in a system when it reaches a state in which no further change is perceptible, no matter how long one waits (Pippard, 1981). This could happen if the system sinks into a very deep free energy minimum. Whether this represents the lowest free energy state, it is impossible to say, and a question more of philosophy than of practical consequence. It is more appropriate to refer to the state of metastable equilibrium, which represents a local minimum in free energy but does not exclude the existence of other deeper minima. The laws governing metastable equilibria are exactly identical to those dealing with equilibrium so this procedure has no obvious difficulties.

A bainitic microstructure is far from equilibrium. The free energy change accompanying the formation of bainite in an Fe-0.1C wt% alloy at 540 °C is  $-580\text{J mol}^{-1}$ , whereas that for the formation of an equilibrium mixture of allotriomorphic ferrite and austenite at the same temperature is  $-1050\text{J mol}^{-1}$ . Consequently, the excess energy of bainite is some  $470\text{J mol}^{-1}$  relative to allotriomorphic ferrite, equivalent to about 0.04 in units of  $RT_M$ , where  $R$  is the Gas Constant and  $T_M$  the absolute melting-temperature. This is about an order of magnitude larger than the stored energy of a severely deformed pure metal. It is small, however, when compared against highly metastable materials such as rapidly-quenched liquids which solidify as supersaturated solutions, or multilayered structures containing a large density of interfaces (Table 5.1). Thus, bainitic steels can be welded whereas all the other materials listed with higher stored energies would not survive the welding process.

The concepts of equilibrium, metastable equilibrium and indeed, constrained equilibrium, remain useful in spite of the large excess energies. For bainite, we shall apply them in the interpretation of the mechanism of transformation and obtain results which are of very great importance in the design of modern steels.

**Table 5.1** Excess energies of metastable materials; adapted from Turnbull (1981)

Example	Excess energy $RT_M$
Highly supersaturated solution	1
Amorphous solid	0.5
Artificial multilayers	0.1
Bainite	0.04
Cold-deformed metal	0.003

## 5.2 Chemical Potential

Pure iron can exist in many allotropic forms including ferrite ( $\alpha$ ) and austenite ( $\gamma$ ). These two phases can be said to be in equilibrium when their molar Gibbs free energies are identical;

$$G_m^\alpha = G_m^\gamma \quad (5.1)$$

There is then no net tendency for atoms to transfer from one allotrope to the other, because the free energy of the iron atom in  $\alpha$  is precisely equal to that in  $\gamma$ .

Similarly, for an iron–carbon solid solution, equilibrium is when there is no net tendency for either iron or carbon atoms to transfer between ferrite and austenite, even though the two phases may differ in composition. That is, the free energy of a carbon (or iron) atom must be identical in ferrite and in austenite at equilibrium. It is no longer the case that the ferrite and austenite have identical free energies at equilibrium.

It therefore becomes useful when considering the thermodynamics of solid solutions to partition the free energy of phase into parts which are attributed to the individual components. This leads to the concept of a chemical potential. The molar Gibbs free energy of a binary solution can be written as a weighted average of its components  $A$  and  $B$ :

$$G_m = x_A\mu_A + x_B\mu_B \quad (5.2)$$

where  $\mu_i$  is the chemical potential of element  $i$  in a solution where its concentration is  $x_i$ . This equation is represented graphically in Fig. 5.1, from which it can be seen that the chemical potential  $\mu_A$  of  $A$  can be interpreted simply to represent the average free energy of a mole of  $A$  atoms *in a solution* of composition  $x_A$ .

Equilibrium is said to exist between homogeneous phases when the chemical potential  $\mu_i$  of each component  $i$  is the same in all the phases present:

$$\mu_i^\gamma = \mu_i^\alpha \quad \text{for all } i. \quad (5.3)$$

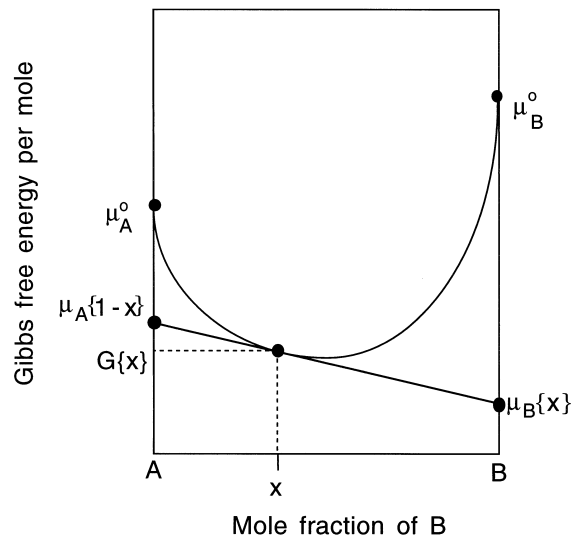


**Fig. 5.1** The chemical potentials  $\mu_A$  and  $\mu_B$  for components  $A$  and  $B$  respectively, in a solution containing a mole fraction  $x$  of  $B$  and  $1 - x$  of  $A$ . The potentials are given by the intercepts on the vertical axes of the tangent drawn at  $x$  to the curve representing the solution free energy.  $\mu_A^0$  and  $\mu_B^0$  are the molar Gibbs free energies of pure  $A$  and  $B$  respectively.

This is illustrated in Fig. 5.2, which shows that the equilibrium compositions  $x^{\alpha\gamma}$  and  $x^{\gamma\alpha}$  of ferrite and austenite respectively, can be determined by constructing a tangent which is common to both the free energy curves. The intercept of the tangent with the vertical axes gives the chemical potentials, which are identical for each species whatever the phase, by virtue of the fact that the tangent is common.

The concept of equilibrium in terms of phases which are *homogeneous* is rather restrictive. Instead, it is useful to consider equilibrium to exist locally. For example, it is a reasonable approximation that during diffusion-controlled growth, the compositions of the phases in contact at the interface are such as to allow equilibrium to exist locally even though there may be concentration gradients in the matrix ahead of the interface. As long as the phases are not too inhomogeneous, as with some artificial multilayered structures or during spinodal decomposition, classical equilibrium thermodynamics can be applied locally without raising any fundamental difficulties.

A form of constrained equilibrium which arises in substitutionally alloyed steels is *paraequilibrium*, in which the ratio of iron to substitutional solute atoms remains the same everywhere, but subject to that constraint, the carbon atoms achieve a uniform chemical potential at all locations (Fig. 2.11). Either the substitutional solute atoms, or the iron atoms are then trapped by the advan-

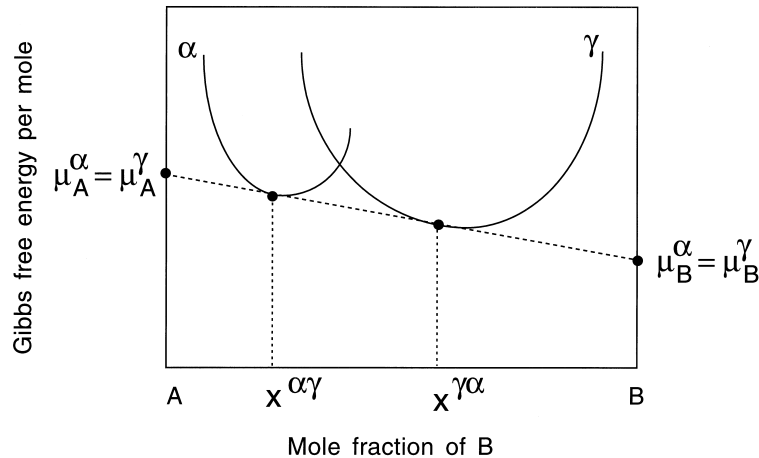


**Fig. 5.2** The common tangent construction which defines the equilibrium chemical compositions of the the  $\alpha$  and  $\gamma$ .

cing transformation interface. An atom is said to be trapped when its chemical potential increases on transfer across the interface.

Transformation can occur without any composition change at a temperature below  $T_0$ , where the parent and product phases of identical composition have equal free energy (Fig. 1.4).

The concepts of local equilibrium, paraequilibrium and transformation without any change in composition are easy to visualise and formulate. However, between the states of local and paraequilibrium, there can in principle exist an infinite number of alternatives in which the substitutional solutes partly partition between the phases. There may similarly be a gradation between paraequilibrium and composition-invariant transformation in which the extent to which carbon is partitioned may vary. Such intermediate states would have to be stabilised by some other rate-controlling factor such as interface kinetics. They would otherwise tend towards equilibrium, because any perturbation which leads to a reduction in free energy would be stable. We shall see in Chapter 6 that the stabilisation of such nonequilibrium states is in certain circumstances possible for solid-state transformations in steels.

### 5.3 Stored Energy due to Transformation

Much of the stored energy of bainite comes from the distortions due to the shape deformation accompanying transformation. For a plate in the form of an oblate ellipsoid of semi-axes  $R$ ,  $R$  and  $y$ , with  $R \gg y$ , the strain energy per mole is given by (Christian, 1958):

*Thermodynamics*

$$G_s = \frac{\mu V_m}{1 - \nu} \left[ \frac{2}{9} (1 + \nu) \Delta^2 + \frac{\pi y}{4R} \zeta^2 + \frac{(1 - \nu) \pi y}{3R} \Delta \zeta \right] + \frac{1}{2} \mu V_m \frac{(2 - \nu) \pi y}{4(1 - \nu) R} s^2 \quad (5.4)$$

where  $\mu$  and  $\nu$  are the shear modulus and Poisson's ratio respectively of the surrounding matrix,  $V_m$  is the molar volume of the matrix,  $\Delta$  is the uniform dilatation accompanying transformation,  $\zeta$  is the additional uniaxial dilatation normal to the habit plane and  $s$  is the shear component of the shape change (Fig. 5.3).

The uniform dilatation  $\Delta$  term has been used to interpret the crystallography of bainite but its existence has not been confirmed by measurements and so it is neglected in further discussions. The energy due to the shear and  $\zeta$  strains comes to about  $400 \text{ J mol}^{-1}$  for bainite (Bhadeshia, 1981a). This is less than the corresponding term for martensite, which is about  $600 \text{ J mol}^{-1}$  because bainite plates usually have a smaller aspect ratio ( $y/R$ ). The shear and dilatational components of the shape change are similar for martensite and bainite.

The stored energy of  $400 \text{ J mol}^{-1}$  applies strictly to an isolated plate of bainite which is elastically accommodated in the surrounding austenite. However, bainite grows as clusters of plates and it may be more appropriate to consider the sheaf as a whole, in which case the stored energy may be reduced by averaging the shear over the thickness of the sheaf in which the bainite plates are separated by intervening films of austenite or other phases.

The strain energy can be reduced by plastic relaxation. This is particularly relevant for bainite because the yield strength of austenite is reduced at high temperatures. The plastic deformation causes an increase in dislocation density, but since the deformation is driven by the shape change, the strain energy calculated on the basis of an elastically accommodated shape change should be an upper limit (Christian, 1979b). There may also be a reduction in the stored

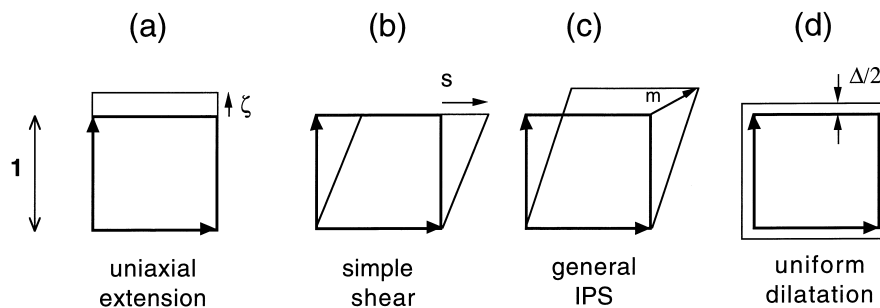


**Fig. 5.3** The strains used in equation 5.4. (a) Uniaxial dilatation normal to the habit plane; (b) shear parallel to the habit plane; (c) a combination of shear and uniaxial dilatation which defines the invariant-plane strain (IPS) which is the shape deformation associated with bainite; (d) uniform dilatation.

energy per unit volume as transformation proceeds because of the tendency of adjacent sheaves to grow in mutually accommodating formations (Hehemann, 1970).

In martensitic reactions, transformation twinning can contribute about  $100 \text{ J mol}^{-1}$  of stored energy; this is not applicable to bainite where the lattice-invariant shear is presumed to be slip.

## 5.4 Thermodynamics of Growth

### 5.4.1 *Substitutional Solutes during Growth*

The atom-probe experiments described in Chapter 2 have established that there is no redistribution of substitutional solutes during the bainite transformation. These experiments cover the finest conceivable scale for chemical analysis. They rule out any mechanism which requires the diffusion of substitutional solutes. This includes the local equilibrium modes of growth.

By contrast, all experimental data show that pearlite grows with the diffusion of substitutional solute atoms (Ridley, 1984, Al-Salman and Ridley, 1984). Chromium, molybdenum, silicon and cobalt have been shown to partition at the reaction front. The extent of partitioning is smaller for manganese and nickel, especially at large undercoolings, but there is localised diffusion (Hillert, 1982; Ridley, 1984). These observations are expected because pearlite is the classic example of a reconstructive transformation.

Solute in iron affect the relative stabilities of austenite and ferrite. This thermodynamic effect is identical for all transformations. We have seen, however, that substitutional solutes do not diffuse at all during displacive transformations whereas they are required to do so during reconstructive transformation. It is for this reason that the observed effect of solutes, on the rate of transformation, is larger for reconstructive than for displacive transformations (Fig. 5.4).

### 5.4.2 *Interstitial Solutes during Growth*

It is simple to establish that martensitic transformation is diffusionless, by measuring the phase compositions before and after transformation. Bainite forms at somewhat higher temperatures where the carbon can escape out of the plate within a fraction of a second. Its original composition cannot therefore be measured directly.

There are three possibilities. The carbon may partition during growth so that the ferrite may never contain any excess carbon. The growth may on the other hand be diffusionless with carbon being trapped by the advancing interface.

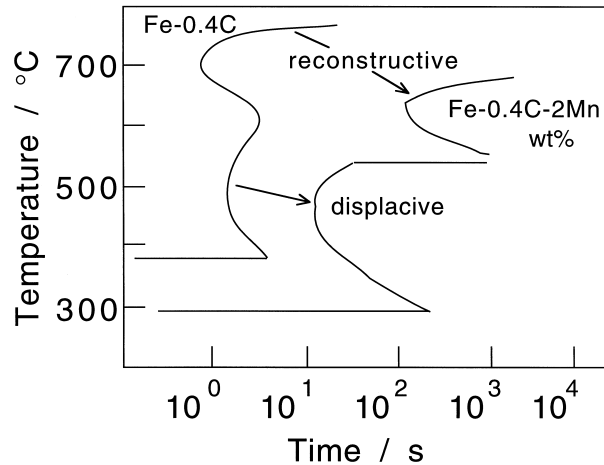


**Fig. 5.4** Time-temperature-transformation diagrams showing the larger retarding effect that manganese has on a reconstructive transformation compared with its influence on a displacive transformation.

Finally, there is an intermediate case in which some carbon may diffuse with the remainder being trapped to leave the ferrite partially supersaturated.

Diffusionless growth requires that transformation occurs at a temperature below  $T_0$ , when the free energy of bainite becomes less than that of austenite of the same composition. Growth without diffusion can only occur if the carbon concentration of the austenite lies to the left of the  $T_0$  curve (Fig. 1.4).

Suppose that the plate of bainite forms without diffusion, but that any excess carbon is soon afterwards rejected into the residual austenite. The next plate of bainite then has to grow from carbon-enriched austenite (Fig. 5.5a). This process must cease when the austenite carbon concentration reaches the  $T_0$  curve. The reaction is said to be incomplete, since the austenite has not achieved its equilibrium composition given by the  $Ae_3$  phase boundary. If on the other hand, the ferrite grows with an equilibrium carbon concentration then the transformation should cease when the austenite carbon concentration reaches the  $Ae_3$  curve.

It is found experimentally that the transformation to bainite does indeed stop at the  $T_0$  boundary (Fig. 5.5b). The balance of the evidence is that the growth of bainite below the  $B_S$  temperature involves the successive nucleation and martensitic growth of sub-units, followed in upper bainite by the diffusion of carbon into the surrounding austenite. The possibility that a small fraction of the carbon is nevertheless partitioned during growth cannot entirely be ruled out, but there is little doubt that the bainite is at first substantially supersaturated with carbon.

### Bainite in Steels

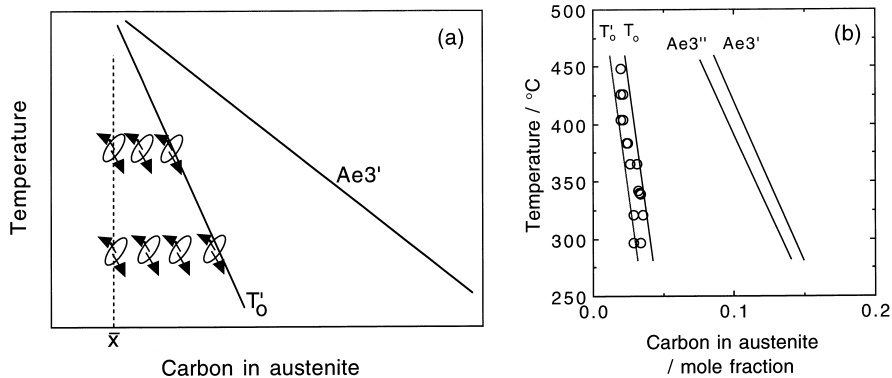


**Fig. 5.5** The incomplete-reaction phenomenon. A plate of bainite grows without diffusion, then partitions its excess carbon into the residual austenite. The next plate thus grows from carbon-enriched austenite. This process can only continue until  $x_\gamma = x'_{T_0}$ . For paraequilibrium growth, the transformation should proceed until the carbon concentration reaches the  $Ae_3''$  curve. (b) Experimental data on the incomplete reaction phenomenon for Fe-0.43C-3Mn-2.12Si wt% alloy (Bhadeshia and Edmonds, 1979a).

The chemical potentials are not uniform in the steel when the bainite reaction stops. The reaction remains incomplete in that the fraction of bainite is less than expected from a consideration of equilibrium between austenite and ferrite. The carbon concentration of the austenite at the point where the bainite reaction stops is far less than given by the  $Ae_3''$  phase boundary.<sup>†</sup> This 'incomplete reaction phenomenon' explains why the degree of transformation to bainite is zero at the  $B_S$  temperature and increases with undercooling below  $B_S$  in steels where other reactions do not overlap with the formation of bainitic ferrite. The  $T'_0$  curve has a negative slope on a temperature/carbon concentration plot, permitting the austenite to accommodate ever more carbon at lower temperatures.

The experimental evidence for the incomplete reaction phenomenon comes in many forms. The carbon concentration of the residual austenite at the point where the reaction stops has been measured using X-ray techniques, lattice imaging using high resolution transmission electron microscopy, field ion microscopy/atom probe methods, quantitative metallography and dilatometry. Real time neutron transmission experiments have also demonstrated the effect (Meggers *et al.*, 1994). It is always found that the concentration is far below that required by equilibrium or paraequilibrium, and is on the whole

<sup>†</sup> $Ae_3'$  refers to the paraequilibrium  $(\alpha + \gamma)/\gamma$  phase boundary.  $Ae_3''$  is the corresponding boundary allowing for the stored energy of bainite.



consistent with that given by the  $T'_0$  curve of the phase diagram. The experimental evidence has been reviewed by Christian and Edmonds (1984). In dilatometric experiments, the length change due to transformation is zero above the  $B_S$  temperature, even though that temperature may be well within the  $\gamma + \alpha$  phase field. The maximum length change then increases with undercooling below the  $B_S$  temperature. Numerous examples of the type illustrated in Fig. 5.6 can be found in the published literature.

The failure of the bainite reaction to reach completion reveals the role of carbon during transformation. An important consequence is that the  $T_0$  curve can be used in the design of steels. In the context of bainite, the curve gives the limiting carbon concentration  $x_{T'_0}$  of the austenite, a parameter of enormous importance in devising microstructures containing stable austenite. A discussion of the procedure is deferred to Chapters 12, 13, but Fig. 5.7 illustrates the remarkable predictive ability of the concept for a large variety of steels. By contrast, the  $Ae3'$  phase boundary gives very poor estimates of the austenite composition in the context of bainite.

The incomplete transformation leaves films of austenite between bainite plates. These films improve the properties of steels. It has been found that the thickness of these austenite films can be estimated by assuming that the carbon diffusion field around an existing plate of ferrite prevents the close approach of another parallel plate. This is because the regions of austenite with the highest carbon concentration (i.e.  $x_\gamma > x_{T'_0}$ ) are unable to transform

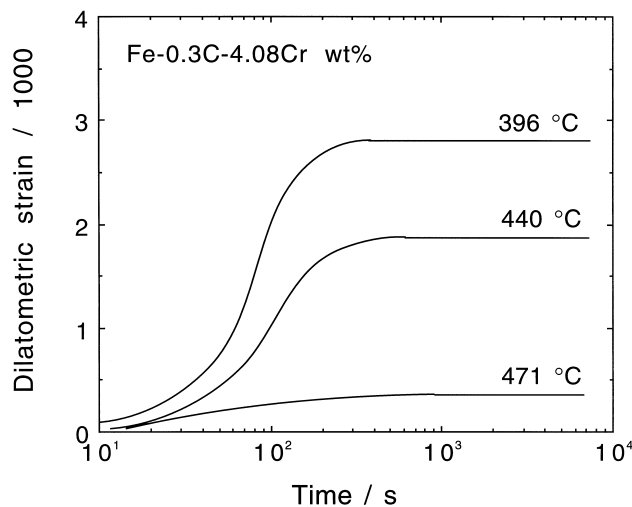


**Fig. 5.6** Dilatometric length change data illustrating the incomplete reaction phenomenon for a Fe-0.3C-4.08Cr wt% alloy (Bhadeshia, 1981b).

## Bainite in Steels

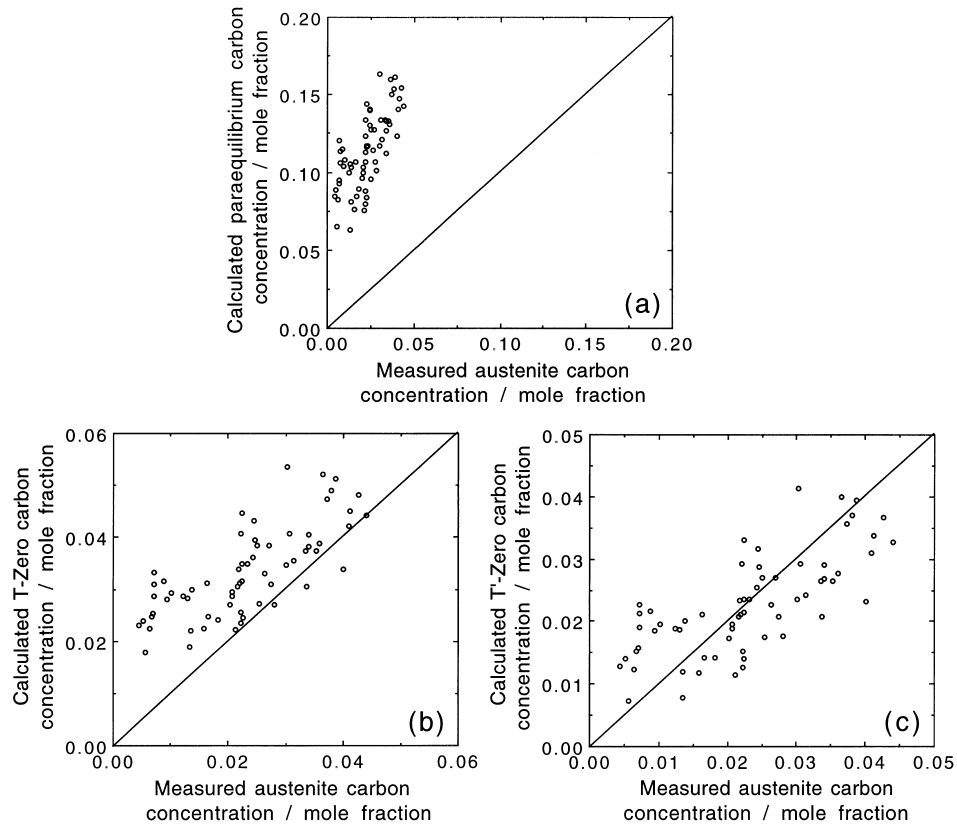


**Fig. 5.7** A comparison of the measured carbon concentration of the austenite which remains untransformed when the bainite reaction stops, versus that calculated using the  $Ae3'$ ,  $T_0$  and  $T'_0$  criteria. After Chang and Bhadeshia (1995).

to bainite (Fig. 5.8). This simple theory predicts a dependence of film thickness on the bainite plate thickness since the net quantity of carbon partitioned into the austenite must increase with the thickness of the bainite plate. The correlation can be seen in Fig. 5.8c. Note that a better fit is seen in Fig. 5.8b because those calculations include both the plate thickness and the effects of alloying elements on the  $T'_0$  condition.

### 5.4.3 Approach to Equilibrium

Although the bainite reaction stops before equilibrium is reached, the remaining austenite can continue to decompose by reconstructive transformation, albeit at a greatly reduced rate. Pearlite often forms sluggishly after bainite. The delay between the cessation of bainite and the start of pearlite varies with

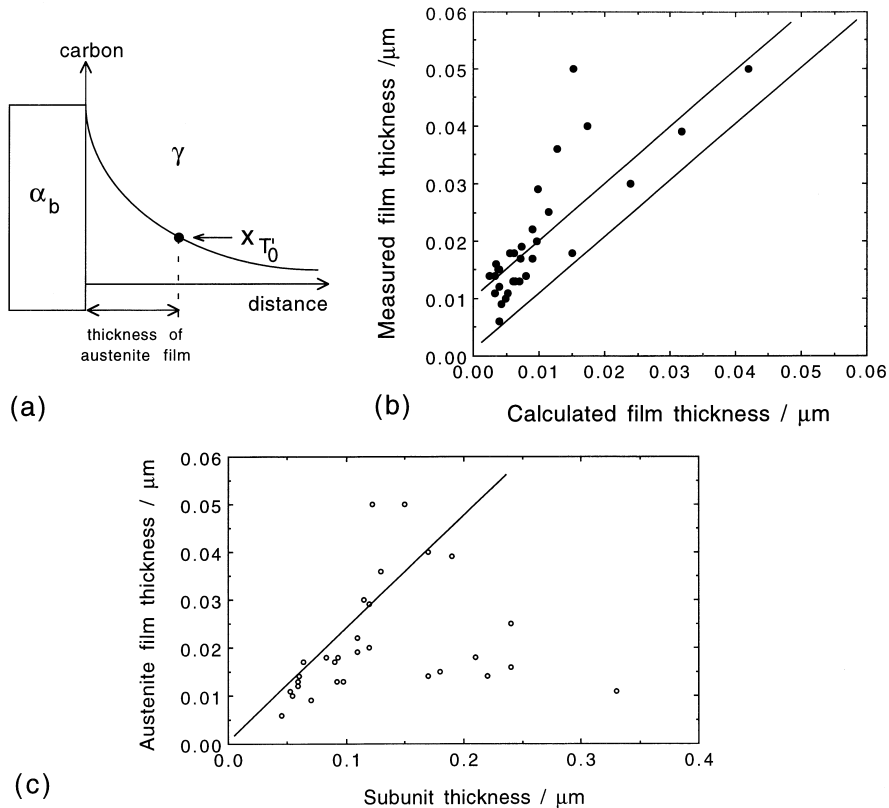


**Fig. 5.8** (a) The thickness of the austenite film is determined by the point where the carbon concentration in the residual austenite is  $x_{T_0}$ . (b) Comparison of measured and calculated austenite film thicknesses for a variety of alloys. (c) Austenite film thickness versus that of the adjacent bainite sub-unit (Chang and Bhadeshia, 1995).

the steel composition and transformation temperature. In one example the bainite reaction stopped in a matter of minutes, with pearlite growing from the residual austenite after some 32 h at the transformation temperature of 450 °C. In another example, isothermal reaction to lower bainite at 478 °C was completed within 30 min, but continued heat treatment for 43 days caused the incredibly slow reconstructive transformation to two different products. One of these was alloy-pearlite which nucleated at the austenite grain boundaries and which developed as a separate reaction (Fig. 4.5a). The other involved the irregular, epitaxial and reconstructive growth of ferrite from the existing bainite. The extent of ferrite growth in 43 days was comparable to the thickness

of the bainite plates, which took just a few seconds to form (Bhadeshia, 1981b, 1982b).

The two-stage decomposition of austenite is more difficult to establish for plain carbon steels where the reaction rates are large, with the pearlite reaction occurring a few seconds after bainite (Klier and Lyman, 1944).

## 5.5 Summary

The thermodynamic description of the bainite reaction is linked to its mechanism of growth and depends on the behaviour of solute atoms during transformation. By far the largest contribution to the stored energy of bainite is due to the invariant-plane strain shape deformation. The contributions from interfacial area are by comparison negligible during the growth stage. The dislocation density of bainite has its origins in the plastic accommodation of the shape change. The energy of the dislocations is therefore already accounted for in the estimate of an elastically accommodated shape change.

Substitutional solutes do not partition at all during the bainite reaction. Their primary effect is through their influence on the relative thermodynamic stabilities of the austenite and ferrite phases. The trapping of solutes in the bainite raises its free energy.

The fact that the transformation stops well before equilibrium is achieved is consistent with a mechanism in which growth is diffusionless, although the carbon atoms are partitioned soon afterwards from supersaturated ferrite.